Erosion Modeling for the Clive DU PA

Clive DU PA Model v1.2

8 July 2014

Prepared by

NEPTUNE AND COMPANY, INC.

1505 15th St, Suite B, Los Alamos, NM 87544

1. Title: Erosion Modeling for the Clive DU PA		
2. Filename: Erosion Modeling v1.2.docx		
3. Description: This white paper provides documentation of the development of parameter values and distributions used for modeling erosion for the Clive DU PA Model v1.2.		
	Name	Date
4. Originator	Michael Sully	17 May 2014
5. Reviewer	Dan Levitt, John Tauxe	27 May 2014
6. Remarks 17 May 2014: Added documentation of new erosion modeling approach from the SIBERIA modeling of the borrow pit. – M. Sully 21 May 2014: Major reorganization and accepted track change edits. – Dan Levitt 27 May 2014: Minor edits, clean up for formatting and style, redrafting of many equations. – John Tauxe 4 July 2014: Revisions for Round 3. – M. Sully		

This page is intentionally blank, aside from this statement.

CONTENTS

FIGURES

TABLES

1.0   Erosion Model Input Distribution Summary

A summary of parameter values and distributions employed in the erosion modeling component of the Clive Depleted Uranium Performance Assessment Model (the Clive DU PA Model) is provided in Table 1. Additional information on the derivation and basis for these inputs is provided in subsequent sections of this report.

For distributions, the following notation is used:

- N(μ, σ, [*min*, *max*]) represents a normal distribution with mean μ and standard deviation σ, and optional truncation at the specified *min*imum and *max*imum,
- LN(*GM*, *GSD*, [*min*, *max*]) represents a log-normal distribution with geometric mean *GM* and geometric standard deviation *GSD*, and optional *min* and *max*,
- U(*min*, *max*) represents a uniform distribution with lower bound *min* and upper bound *max*,
- Beta(μ, σ, *min*, *max*) represents a generalized beta distribution with mean μ, standard deviation σ, minimum *min*, and maximum *max*,
- Gamma(μ, σ) represents a gamma distribution with mean μ and standard deviation σ, and
- TRI(*min*, *m*, *max*) represents a triangular distribution with lower bound *min*, mode *m*, and upper bound *max*.

Table 1. Summary of distributions for erosion modeling

GoldSim Model Parameter	Symbol	Units	Distribution or Value	Notes
Gully_b_parameter	b	—	normal(μ = -0.4, σ = 0.15, min = -0.75, max = -0.05)	See Section 5.3.1
L_init	L_0	m	uniform(Small, 5)	See Section 5.2
AngleOfRepose_Gully	$α_{gully}$	deg	normal(μ = 38, σ = 5, min = Small, max = 90 − Small)	Clover, 1998 (for gravel); See Section 5.2
AngleOfRepose_Fan	$α_{fan}$	deg	uniform(5, 10)	See Section 5.2
Number_of_Gullies		—	Discrete uniform(min=1, max=20)	See Section 5.1 and Section 5.4
ConvergenceCriterion		m^3	0.01	modeling construct
FractionGully	—	—	A Table of 1000 generated values	See Section 4.2

2.0   Introduction

The safe storage and disposal of depleted uranium (DU) waste is essential for mitigating releases of radioactive materials and reducing exposures to humans and the environment. Currently, a radioactive waste facility located in Clive, Utah (the "Clive facility") operated by Energy*Solutions* is being considered to dispose DU waste that has been declared surplus by the U.S. Department of Energy (DOE). The Clive facility has been tasked with disposing of the DU waste in a manner that protects humans and the environment from future radiological releases.

To assess whether the proposed Clive facility location and containment technologies are suitable for protection of human health, specific performance objectives for land disposal of radioactive waste set forth in Utah Administrative Code (UAC) Rule R313-25 *License Requirements for Land Disposal of Radioactive Waste - General Provisions* must be met—specifically R313-25-8 *Technical Analyses*. In order to support the required radiological performance assessment (PA), a probabilistic computer model has been developed to evaluate the doses to human receptors and concentrations in groundwater that would result from the disposal of radioactive waste, and conversely to determine how much DU waste can be safely disposed at the Clive facility. The GoldSim systems analysis software (GTG, 2010) was used to construct the probabilistic Clive DU PA Model.

The site conditions, chemical and radiological characteristics of the wastes, contaminant transport pathways, and potential human receptors and exposure pathways at the Clive facility that are used to structure the Model are described in the conceptual site model (CSM) documented in the *Conceptual Site Model* white paper (Clive DU PA CSM.pdf).

The purpose of this white paper is to address specific details of the erosional processes that may affect cover performance. This paper is organized to give a brief overview of erosional processes, present the overall modeling approach and assumptions, followed by the presentation of the mathematical formulae that are used to represent these processes in the Clive DU PA Model.

Above-ground covers of waste repositories are subject to erosion by the forces of wind and water. The proposed waste disposal cell for DU at the Clive facility, which has an engineered above-ground cover, is subject to these erosional processes. Both wind and water erosion are represented in the Clive DU PA Model. Details of wind erosion modeling and the effects on dose to potential receptors are addressed in detail in the *Atmospheric Transport Modeling* white paper, (Atmospheric Modeling.pdf) and are not addressed further in this white paper. Water erosion via the return of Lake Bonneville or a small lake is not discussed in this document, but is addressed in the *Deep Time Assessment* (Deep Time Assessment.pdf). Other water erosional processes are described below.

There are two types of water erosion in the CSM: sheet erosion and gully erosion (channel formation). Two approaches have been used in the Clive DU PA Model to evaluate the influence of erosion on embankment performance. The first uses results from a landscape evolution model of a borrow pit area at the Clive site as an analog for embankment cover erosion and the second applies a gully model in a screening approach to evaluate the effects of the occurrence of gullies. Only the first approach (borrow pit model analog) is currently implemented in the Model,

although the second approach (gully screening model, used in the Clive DU PA Model v1.0) is included in the Model as an optional calculation.

2.1   Sheet Erosion

Sheet erosion is erosion of soil particles by water flowing overland as a "sheet" in a downslope direction. During extremely high rainfall events when rain falls faster than water can infiltrate, runoff can occur, acting as a mechanism for removing/eroding cover materials. Sheet erosion is a uniform process over the area of the cover and depends largely on the magnitude and shape of the slope, soil texture, and cover characteristics, as well as rainfall intensity. This is different from erosion that flows in defined channels (i.e., gully erosion), which is discussed in Section 2.2.

In the top slope of the embankment, where slopes are gradual (about 2% slope), sheet erosion will be slower than on the steeper side slopes of the cell (about 20% slope) (*Embankment Modeling* white paper). As soil and loess move down slope by sheet erosion, it is likely that their volumes would be replenished by deposition of clean loess from the surrounding environs (i.e., a net balance of zero change). In the end, the total soil volume on the embankment would not change, though there would be a slow movement of soils down slope, along with the contaminants they could potentially contain. While both sheet and gully erosion are considered in the Clive DU PA Model (v1.2) little contamination is likely to be transported by sheet erosion, and gully erosion is expected to be far more significant. Sheet erosion likely would have little effect, except possibly to move a small amount of potentially contaminated soil down slope.

2.2   Gully Erosion

Gully erosion is a process that occurs when water flows in narrow channels, particularly during heavy rainfall events. Gully erosion typically results in a gully that has an approximate "V" cross section that widens (lateral growth) and deepens (vertical growth) through time until the gully stabilizes. The formation of gullies is a concern on uranium mill tailings sites and other long-term above-ground radioactive waste sites (NRC 2010). Gully erosion has the potential to move substantial quantities of both cover materials and waste, should the waste material be buried close to the surface. It occurs when surface water runoff becomes channeled and repeatedly removes soil along drainage lines, creating a depositional fan of the removed materials.

There are two important features of the gully that need to be considered when modeling gully erosion: the thalweg and the angle of repose. The thalweg is a line that joins the lowest points of the gully along the entire length of the gully, defining the gully's deepest channel. It can conceptually be thought of as the bottom of the gully that runs along a downward slope. The angle of repose is the angle the side of the gully makes with the horizontal; it is a property of the material that is eroding.

The engineered cover at the Clive facility may be subject to gully erosion via a disturbance attributed to an animal burrow, large animal tracks, the root of a fallen tree or shrub (root throw), or off-highway vehicle (OHV) track. It is assumed that a notch or nick will be created from these activities at some location on the surface of the cover and the feedback processes inherent in gully formation will cause erosion downward to the surrounding grade and erosion upward

toward the top slope of the embankment. As water flows across the inner walls of the notch, erodible solid materials will be transported with it, creating a larger notch (both vertically and laterally) and thus a greater capacity to remove solid material. As this process continues, more material will erode down-gradient from the notch, as well as up-gradient from the notch. Also, as water flows down the thalweg it can undercut the gully banks, causing materials to slump into the thalweg, where they get washed along the downward slope until the angle of repose is reached. A wedge-shaped volume of material is removed and deposited on the neighboring flat as a sort of small alluvial fan, forming its own angle of repose. This process continues until the mouth of the gully has met the top of the removed material. Gully erosion was evaluated as having the potential to occur at the Clive facility and is included using two approaches (described above) for the Clive DU PA Model.

In the GoldSim implementation of gully erosion, a gully is assumed to form (via rainfall, etc.) after the initiating event of an OHV disturbing the rip-rap outer cover material; i.e., the OHVs are only initiating the gullies. The gullies that are modeled are deeply-incised to the extent that they reach the waste layers with side walls at the angle of repose and a wedge shape with a narrow top and broader base where the gully meets the level grade surrounding the disposal cell. The steep-walled profile of the eventual deeply-incised and narrow gullies would likely preclude extensive OHV activity in the gullies themselves; i.e., once a gully forms, OHV users (if any) would likely ride elsewhere on the cover. Thus, the use of area-average embankment air and soil concentrations in the Dose Container for OHV user exposure across the entire disposal unit, including gullies, is appropriate and likely to be protective.

3.0 Evapotranspiration Cover Design

The composition of the embankment cover is an important factor in determining its erodibility. At the Clive facility, the cover for the portion of the Federal Cell housing DU (the Federal DU Cell) is an evapotranspiration (ET) cover composed of a 6-in. thick Surface Layer of native vegetated Unit 4 material with 15 percent gravel mixture on the top slope and 50 percent gravel mixture for the side slope. The functions of this layer are to control runoff, minimize erosion, and maximize water loss from ET. This layer of silty clay provides storage for water accumulating from precipitation events, enhances losses due to evaporation, and provides a rooting zone for plants that will further decrease the water available for downward movement. Underlying the surface layer is the Evaporative Zone Layer. This layer is also composed of Unit 4 material and is 12 in. thick. The purpose of this layer to provide additional storage for precipitation and additional depth for plant rooting zone to maximize ET. The Frost Protection Layer is below the Evaporative Zone Layer, and is 18 in. thick. The purpose of this layer is to protect layers below from freeze/thaw cycles, wetting/drying cycles, and inhibit plant, animal, or human intrusion.

For further details on the Federal DU Cell, refer to the *Embankment Modeling* white paper, and for details on ET cover modeling, refer to the *Unsaturated Zone Modeling* white paper.

4.0   Borrow Pit Model Analog

4.1   Simulation of Sheet and Channel Erosion

Landscape evolution models were developed and applied for a face of a borrow pit at the Clive Site in order to predict the response of the pit face and upslope land surface to water erosion processes during runoff events. The models provide a quantitative description of the evolution of slopes and channels (also called gullies in this white paper) over time. The objective of the models was to provide a realistic estimate of the rate of progression of hillslope erosion loss and channel development towards the existing embankments that encase waste. The landscape evolution model SIBERIA (Willgoose, 2005) was selected for this analysis. Landscape evolution models such as SIBERIA capture the interaction between the runoff response and the elevation changes of the landform surface over long time periods. This capability makes models such as SIBERIA particularly well-suited for waste site modeling. The model domain for the borrow pit included the borrow pit floor, a 3-m (10-ft) high pit face at a 1:1 slope and several hundred meters of ground surface upslope from the pit face at a slope of 0.3 percent. The soil was characterized with properties consistent with the Unit 4 silty clay, and had no vegetation or rock cover. While composed of similar soil the surface layer of the top slope of the ET cover proposed for the Federal DU Cell has a slope of 2 percent, a gravel composition of 15 percent, and will be re-vegetated with a mix of native and non-native species. While the cover top slope has a larger slope of 2 percent as compared with the slope of 0.3 percent for the undisturbed area upslope from the borrow pit face, the top slope characteristics included vegetation and gravel admix that would act to slow erosion and channel formation. Changes in elevation at each node were obtained at 100 y, 500 y, and 1000 y. Simulations were done for two rainfall intensities.

Assumptions for this approach include:

- The geometry of the borrow pit wall and upslope area are sufficiently similar to that of the embankment top slope and side slope that the borrow pit serves as an analog.
- The borrow pit materials (Unit 4) are sufficiently similar to the layers of the embankment (Unit 4 with gravel, Unit 4, and radon barrier clays).
- Surface elevation changes at 10,000 y can be extrapolated from SIBERIA model results from 100 y, 500 y and 1000 y.
- The results at 10,000 y approximate steady state of gullies. This steady state assumption is implemented from time zero in this model.
- The area of waste that is deposited on the fan is the same as the area of waste exposed in the gullies, using projections onto the horizontal plane.
- The excavation of ET Cover cells was not considered in the calculations below for contaminants in the excavated mass from the gully because it was assumed that significantly more contaminant mass was in the waste than in the cover and that the material extracted from the waste layers would be on the top of the fan.

A subset of the borrow pit model domain was selected to represent the cover. The area extended from 50 m downslope from the edge of the embankment to 10 m upslope from the borrow pit face. The model domain was represented by a grid with nodes at equal 0.75-m spacings. Changes in elevation at each node were obtained at 100 y, 500 y, and 1000 y. Simulations were done for

two rainfall intensities. Since only small differences in elevation change were seen between the two rainfall intensities, results for both intensities were combined to provide two estimates of elevation change at each of the three times. The 0.1^{th}, 10th, 20th, and 90th percentiles of the simulated data were calculated at each of the three times. These percentile plots in most cases showed a non-linear relationship between the percentile depth of the area and time.

A square-root function was fit to the 0.1^{th}, 10th, 20th, and 90th percentiles using the general form:

$$f(t) = A \times \sqrt{t} + \text{error}$$

where

> $f(t)$ = percentile depth of the area,
> A = amplitude parameter, and
> t = time.

The error term was assumed to follow a normal distribution. The `nls()` function in the 'stats' package of the software program *R* was used to estimate the *A* parameter and the error term. The four percentile plots used for the fit are shown in Figure 1.

After the percentile curves were fit using the square root function, parameters were randomly drawn from the *A* distributions for three of the curves, and values of the function at 10,000 y were calculated. For each of the 1,000 iterations, a lognormal distribution was estimated from the resulting percentiles. The proportion of the lognormal distribution that fell within each specified depth profile was calculated through simulation. An example iteration is included below for demonstration purposes:

1. Simulate '*A*' values for the 10th, 20th, and 90th percentile regression fits. The fits for the 0.1^{th} percentile were not used for stability reasons. These values might be 1.59, 0.670, and -0.228 respectively.
2. Project the depth value for each of the curves at 10,000 years. For the '*A*' parameters above, these would be 159 mm, 67.0 mm, and -22.8 mm respectively.
3. Fit a lognormal distribution to these projected depth fits. This step involves finding the best geometric mean, geometric standard deviation, and shift parameter (lower bound) for the percentiles above. Because the 10th percentile of the data is really the 90th percentile of 'depth', the percentiles used for fitting are subtracted from 1. So for fitting purposes, the 10th percentile of the data is the 90th percentile of the fitted distribution (and so on).
4. The parameters of the lognormal distribution with the best fit are: $\mu = 3.22$, $\sigma = 1.56$, $\theta = -26.2$. One thousand values from this lognormal distribution are simulated, and the proportion that fall within each depth range are calculated, and saved to a matrix. As a point of reference, the theoretical $10^{th}/80^{th}/90^{th}$ percentiles of this distribution are -22.77, 67.03, and 158.8 respectively. So the lognormal distribution fits very well to these three percentiles (see step 2).
5. The matrix of the 1,000 iterations is output to a .csv file and converted to an MS Excel file.
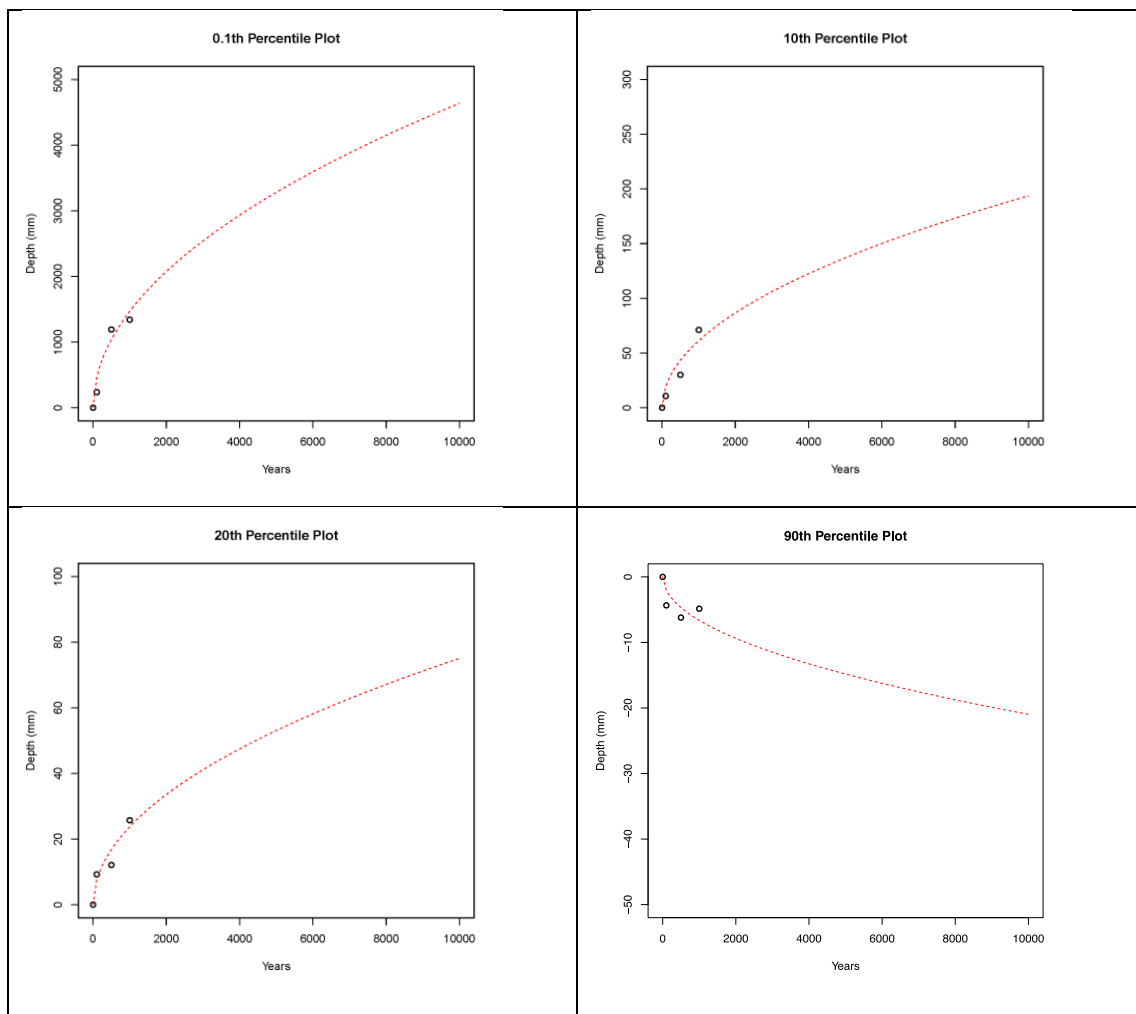
Figure 1. Percentile depth of the area with time and fitted functions.

The first five realizations of fraction of cover area for each elevation change (depth) interval are shown in Figure 2. The original output file included 0.5-m depth increments from the beginning of the waste (1.5 m) up to 10 m. It was clear that there are virtually no gullies greater than 3.5 m, so the depth ranges were cut off there, re-normalized the proportions, and the 3.5-m to 10-m depth ranges were deleted.

The model documentation report and a model package containing the EAMS and SIBERIA software, model input files, grids, and results are provided in an attached electronic addendum.
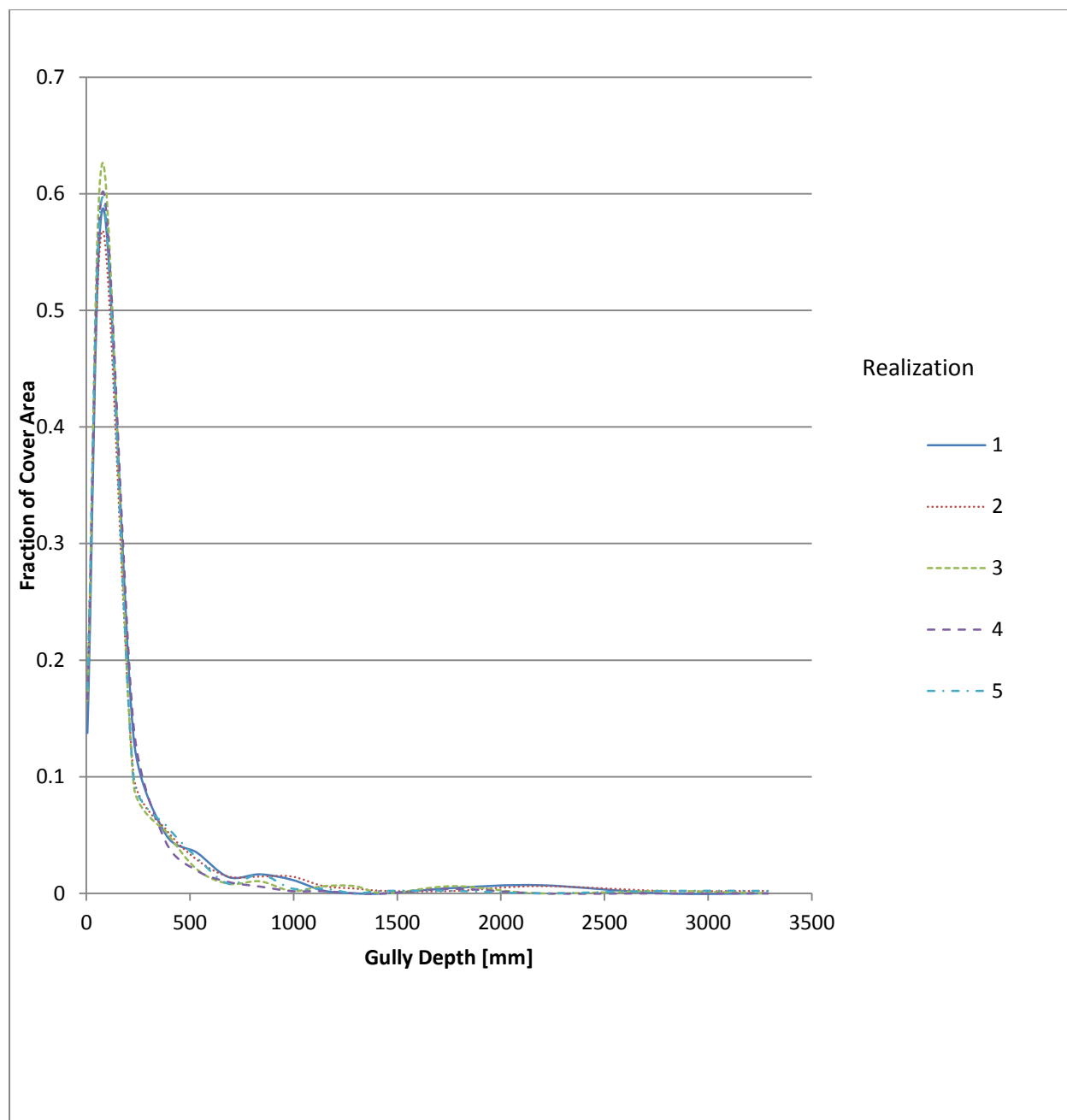
Figure 2. The first five realizations of fraction of cover area for each elevation change (depth) interval.

4.2   Implementation in the Clive DU PA Model

In the Clive DU PA Model, the area of the waste exposed by the gullies and the volume of the waste removed by the gullies are used in the dose calculations. The area of waste exposed by gullies and the resulting fan of waste from gully excavation of the disposal cell is the exposure area for gullies. The volume of the waste removed by gullies is used to calculate a concentration

of radionuclides in the waste that was removed. This concentration of waste is assumed to be spread out over the exposure area of the gullies and fan and is used for dose calculations.

The results in the MS Excel file `SimulatedErosionDepthProportions.xlsx` provide the proportion of area of the cover or waste layer that has a gully "end" at the defined cell depths, where a gully "end" is defined as a cell for which the gully enters in the top of that SIBERIA cell but does not exit out the bottom of the cell. The gully could exit on the side of the cell, but it would still be considered to be an "end" of a gully in that cell as can be seen in the example illustrations in Figure 3 below.

The sum of all the proportions of area is the exposure area for the gullies. The exposure area of the fan is assumed to be the same as the exposure area of the gullies. This assumption is supported by output figures from the SIBERIA model such as the Figure 4 (from the file `5YR_Rainfall_1000YR_Bare.png`.) The fan appears to be similar in size to the area exposed by the gully.

The volume of waste removed by the gully is estimated as the sum of the area above every gully "end" (Figure 3). This assumption is conservative but makes the best estimate available given the level of spatial discretization of the SIBERIA modeling. The volume removed by the gully from each waste layer is multiplied by the concentration of each radionuclide in that waste layer to get the mass of radionuclides removed by the gully over time. The activity mass of radionuclides per mass of soil removed is used in the dose calculations related to gully formation. Note that gully formation in the Clive DU PA Model does not change over time. The gully areas and volumes are fixed for a realization.

Fraction of gully illustration

To clarify the fractions given in the elements FractionWasteCellsGullyEnds and FractionCapCellsGullyEnds, the illustrations are provided below. The fraction of the cap or waste cells in which a gully "ends" was extracted from the SIBERIA output. These fractions denote the proportion of the area in a Cap Cell or Waste Cell for which a SIBERIA modeling cell had a gully enter (from the top) but not exit (from the bottom). The dark gray cells below are the cells that would be counted as having a gully end. The light gray cells are removed in addition to the dark gray cells for volume of gully calculations. Note that because we are counting discrete cells, the area and volume estimates are conservative.

Example 1.

Gully cross-section with grids denoting cells and cell layers in Siberia. The gullies are roughly drawn in as "V"s. The fraction of cells in which the gully "ends", is represented by the dark gray cells. The area of waste exposed by the gullies is that fraction times the surface area of that layer. The volume of waste removed by the gully is the sum of all the cells for which the gully ends (dark gray cells), plus the sum of the cells directly above, represented by light gray cells.
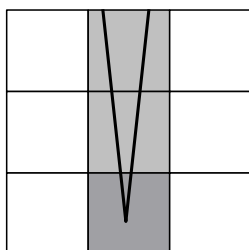
cell layer 1: 0/3 of the cells are counted for the fraction of gully ends;
    1/3 of the cells are removed by gullies for gully volume calculations.

cell layer 2: 0/3 of the cells are counted for the fraction of gully ends;
    1/3 of the cells are removed by gullies for gully volume calculations.

cell layer 3: 1/3 of the cells are counted for the fraction of gully ends;
    1/3 of the cells are removed by gullies for gully volume calculations.

Example 2.

The gully now has "ends" in the first layer since the gully in those cells does not go through to the layer beneath. Thus the fraction of cells in which the gully ends is greater than in Example 1. The volume of the waste removed by the gully similarly increases.
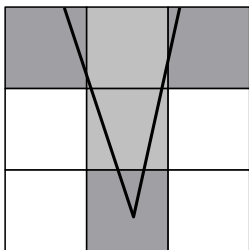
cell layer 1: 2/3 of the cells are counted for the fraction of gully ends;
    3/3 of the cells are removed by gullies for gully volume calculations.

cell layer 2: 0/3 of the cells are counted for the fraction of gully ends;
    1/3 of the cells are removed by gullies for gully volume calculations.

cell layer 3: 1/3 of the cells are counted for the fraction of gully ends;
    1/3 of the cells are removed by gullies for gully volume calculations.
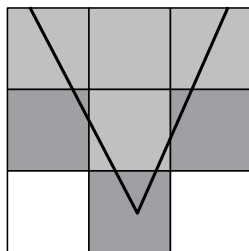
Example 3

This wider gully now has "ends" in the second layer since the gully in those cells does not go through to the layer beneath. Thus the fraction of cells in which the gully ends is greater than in Example 1 or 2. The volume of the waste removed by the gully increases.

cell layer 1: 0/3 of the cells are counted for the fraction of gully ends;
    3/3 of the cells are removed by gullies for gully volume calculations.

cell layer 2: 2/3 of the cells are counted for the fraction of gully ends;
    3/3 of the cells are removed by gullies for gully volume calculations.

cell layer 3: 1/3 of the cells are counted for the fraction of gully ends;
    1/3 of the cells are removed by gullies for gully volume calculations.

Figure 3. Method for estimating gully volume from SIBERIA elevation change results.
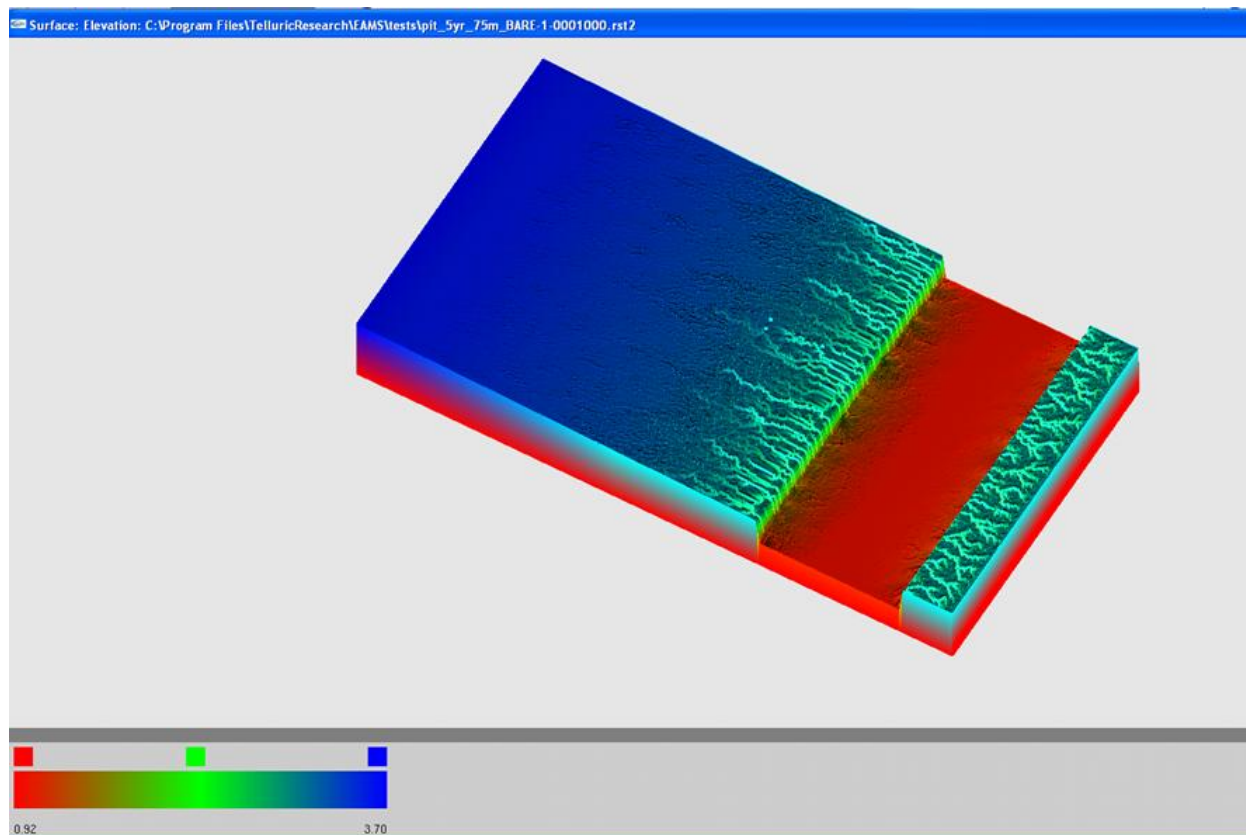
Surface: Elevation: C:\Program Files\TelluricResearch\EAMS\tests\pit_5yr_75m_BARE-1-0001000.rst2

0.92   3.70

Figure 4. Visualization of SIBERIA model simulation of elevation change for bare soil case for the borrow pit at 1000 years.
Vertical exaggeration is 18× making the pit face appear nearly vertical.

5.0 Screening Gully Model

5.1 Screening Gully Model Assumptions

In the development of the erosion modeling approach, Dr. Garry Willgoose, a geomorphologist with expertise in gully formation at The University of Newcastle, Australia, was consulted for advice relating to the modeling of gully formation at the Clive Site. Dr Willgoose is author of the erosion model SIBERIA (Willgoose, 2005) and has experience with gully formation on uranium mill tailings (Willgoose, 2010; Willgoose and Shermeen, 2006). The purpose of the initial gully model in the Clive DU PA Model is to determine whether gullies and fans are significant contributors to dose and whether a more sophisticated erosion model is needed. A simple screening-type gully model was developed with the advice of Dr. Willgoose. To that end, several simplifying assumptions are made:

- Gullies are assumed to form instantaneously, from the time of loss of institutional control. They do not evolve over time. To provide some understanding of what could happen if gullies were allowed to form at different times, concentrations in the gully material that is moved to the fan changes over time, as if the gully were formed instantaneously at any moment in time. These concentrations are used in the dose assessment. This is the only way that the effects of time are considered in the gully model.
- Gully formation occurs independently of main model processes. For example, processes such as biotic intrusion do not occur in gullies, nor does particle resuspension via wind erosion occur from the gully. In addition, the embankment remains intact – top and side slopes of the waste cell do not change in area or geometry with the formation of gullies.
- A small number of gullies is allowed to form in order to evaluate the effects of more than one gully on dose and on model sensitivity. The distribution for the number of gullies allowed is a discrete uniform distribution from 1 to 20. Each gully has the same geometry for any given model realization.
- Types of gully-initiating events are not modeled. Conceptually, these could be either natural (e.g., animal burrows or root throw) or anthropogenic (e.g., OHV track). It is simply assumed that some triggering event occurs.
- The parameters for angles of repose, which in part dictate the geometry of the gullies, are based on the assumption of a homogenous cover material.
- The cross section of a gully is an inverted isosceles triangle, with the bottom vertex of the triangle following along a curved, downward sloping line that is the bottom of the gully (the thalweg).

As shown in Figure 5, gullies that form in the embankment may be of different depths or slightly different shapes. Thus, a different amount of material may be removed for different realizations, resulting in a different amount of potentially expose waste in different realizations. The first picture in Figure 5 shows the intact embankment, with different color shades demonstrating different layers of the cover and waste. The second picture in Figure 5 illustrates a shallow gully formed so that the gully and fan have equal volumes. It is clear that the height of the fan aligns with the mouth of the gully. The third picture in Figure 5 shows another, deeper gully formed. These gully depictions show the mouth of the gully and the height of the fan aligning, as well as equal volumes of fan and gully.

Gully geometry parameters are simulated probabilistically and are constant over a realization, assuming homogeneous materials. These parameters are then used to calculate the depth and volume of the formed gully. Based on this geometry, the amount of exposed waste is then calculated and included in the dose assessment as a soil concentration across the surface area of the fan and the gully.

The remainder of this document describes gully geometry and the derivation of a simple model of a gully, based on recommendations from Dr. Willgoose, as well as the implementation of this model in the Clive DU PA Model.

section of intact embankment

gully and fan must have equivalent volumes

depth of gully depends on several factors
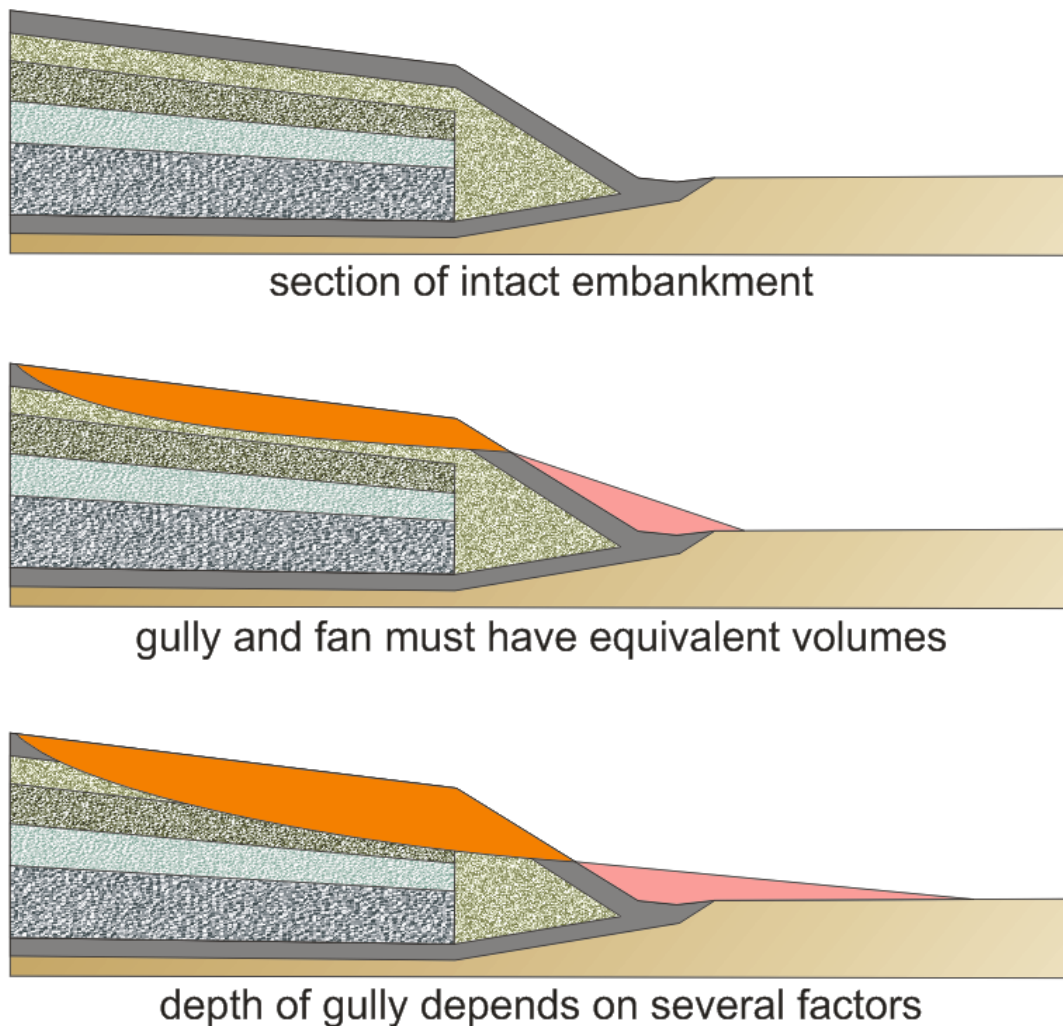
Figure 5. Illustration of the embankment with and without gullies.

5.2   Gully Geometry Overview

The overall geometry of the simplified gully used in the Clive DU PA Model is illustrated in Figure 6. Both Figure 5 and Figure 6 show a representation of half of the embankment, with the ridge of the top slope on the vertical axis. The vertical axis in Figure 6 is the elevation above ground surface, and the horizontal axis is the distance from the ridge of the embankment. The thalweg of the gully is the blue curved line in Figure 6; it forms the bottom of the gully, sloping downward toward the fan.

Figure 6. Longitudinal cross-section of a gully in the embankment.

Any cross section of the gully is assumed to be triangular, with the angle of repose of the gully being the angle that the gully makes 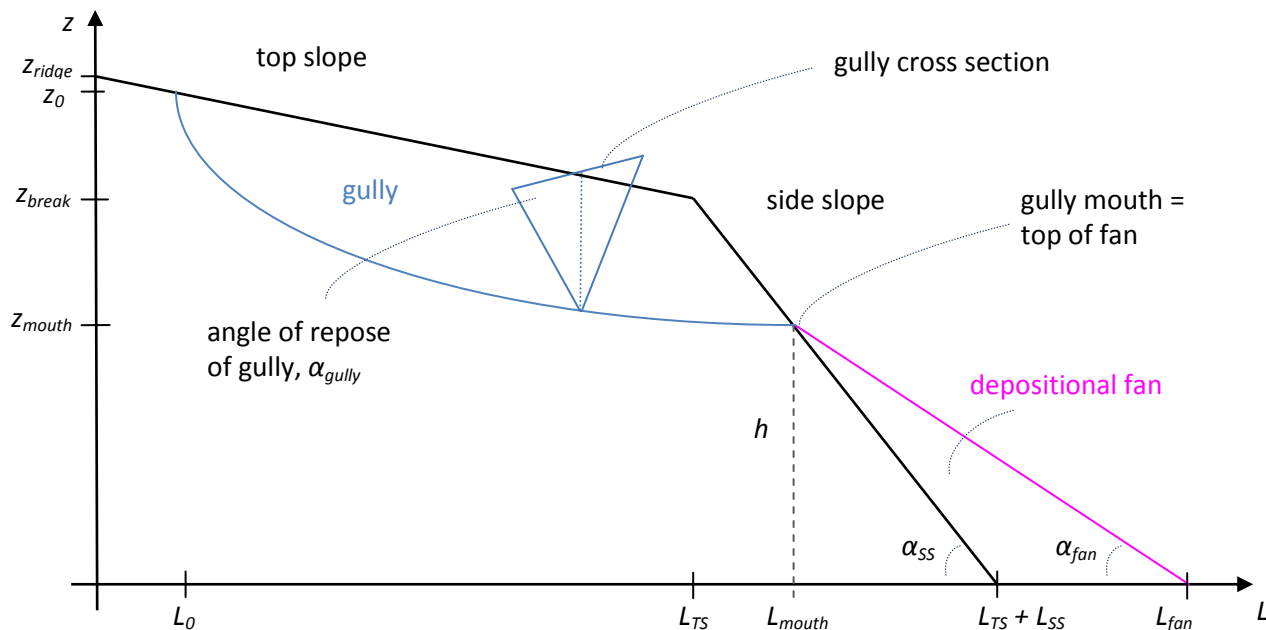with a horizontal plane. The height of the thalweg when it comes out of the embankment through the side slope is also the height of the fan. This parameter, h, is also denoted as z_{mouth}, the elevation of the mouth of the gully. The break in slope is where the top slope and the side slope meet, denoted in Figure 6 by the point (L_{TS}, z_{break}).

The geometry of the gully is fully described by the engineering design of the cover, as described above, and by stochastic parameters for the angle of repose of the gully in the cover material (α_{gully}), the angle of repose of the eroded cover material (α_{fan}), the point of initiation of the gully on the cover (L_0), and the shape parameter of the longitudinal cross section of the gully (b). For these distributions, best professional judgment was used to create reasonably wide distributions that capture uncertainty in these parameters.

The angle of repose of the materials in the gully was represented by choosing values based on gravel, with a mean of 38 degrees, from an estimated range of 30 to 45 degrees (Clover, 1998). A standard deviation of 5 degrees was chosen to allow a slightly wider range of angles, since there is uncertainty in this parameter. Thus a normal distribution was assigned with a mean of 38 degrees, a standard deviation of 5 degrees, a minimum of near zero (10^{-30}) and a maximum of near 90 degrees (90 minus 10^{-30}). The minimum and maximum were chosen by physical constraints.

The gully is assumed to begin less than 2 m from the ridge of the cover (Garry Willgoose, personal communication, 3 Jan 2011). As the point of initiation of the gully gets closer to the ridge, the slope of the gully approaches infinity, so the cover should not start at the ridge itself. In physical terms, the head of the gully stops migrating because there is no significant upslope catchment of water to cause further erosion. A uniform distribution was assigned to L_0, ranging

from near zero (10^{-30}) to 5 m. A gully is not allowed to begin at L_0 equal to zero, exactly at the ridge of the cover; rather, it is kept to one side of the ridge.

The angle of repose of the fan is limited on the high end by the angle created by the side slope and the ground surface, which is about 12 degrees. Since the fan partially lies on top of the side slope, the fan must form a smaller angle. There is some limitation for the smallest angle this fan can form. Considering the large particle size of the gravel and rip rap, it is assumed that the minimum angle of the fan is 5 degrees. So the distribution for α_{fan} is chosen as a uniform distribution from 5 to 10 degrees.

The distribution for *b* is described in Section 5.3.1.

The notation for parameters in Figure 6 is used in the equations below. The following section describes geometry of the gullies as represented by the model and how the dimensions of the gullies are calculated.

5.3   Gully Calculations

The following subsections present the various mathematical formulae for calculating the components of the overall gully model.

5.3.1   Equation for thalweg elevation (gully bottom)

The following form for the slope of the thalweg of the gully as suggested by Dr. Garry Willgoose (personal communication, 3 Jan 2011) is:

$$Slope = \frac{\mathrm{d}z_{gully}}{\mathrm{d}L} = aL^b \,. \qquad (1)$$

where

> z_{gully} is the height of the gully thalweg above natural ground surface,
> L is the horizontal distance from the ridge of the cover downslope,
> a is an amplitude parameter of the steepness of the thalweg slope, and
> b is a dimensionless power parameter, representing the curve of the thalweg.

Conditional on the value of *b*, the value of *a* can be calculated so that the elevation of the mouth of the gully matches the elevation of the fan of material that is washed out of the gully. In order to include the uncertainty in the model, a probability distribution was chosen to represent *b*. A mean value for *b* of -0.4 was estimated from the geomorphology of erosion profiles (Garry Willgoose, personal communication, 3 Jan 2011), and uncertainty about that value was implemented by representing *b* with a truncated normal distribution with a mean of -0.4 and a standard deviation of 0.15, truncated to be between -0.75 and -0.05.

Integrating each side of this equation results in an equation for z_{gully}, the height above ground surface of the thalweg along any point of the thalweg:

$$z_{gully} = \int aL^b \, dL , \text{ and} \tag{2}$$

$$z_{gully} = \frac{a}{b+1} L^{b+1} + C , \tag{3}$$

where

C is the constant of integration.

To find a value for *C*, the point where the gully begins can be used. The top slope of the cover can be represented by the line

$$z_{TS} = \frac{(z_{break} - z_{ridge})}{L_{TS}} L + z_{ridge} . \tag{4}$$

Setting z$_{gully}$ equal to z$_{TS}$ at the start of the gully where $L = L_0$, yields

$$\frac{a}{b+1} L_0^{b+1} + C = \frac{(z_{break} - z_{ridge})}{L_{TS}} L_0 + z_{ridge} . \tag{5}$$

Solving for *C*,

$$C = \frac{(z_{break} - z_{ridge})}{L_{TS}} L_0 + z_{ridge} - \frac{a}{b+1} L_0^{b+1} . \tag{6}$$

In order to simplify this expression, let

$$B_1 = -\frac{1}{b+1} L_0^{b+1} \tag{7}$$

and

$$B_0 = \frac{(z_{break} - z_{ridge})}{L_{TS}} L_0 + z_{ridge} = S_{TS} L_0 + z_{ridge} \tag{8}$$

where

S_{TS} is the slope of the top slope of the cover.

Note that the expression B_0 is the same as the height of the gully where the gully initiates.

Now there is an expression for the elevation of the bottom of the gully (z_{gully}) in terms of the distance from the ridge of the cover:

$$z_{gully} = \frac{a}{b+1} L^{b+1} - B_1 a + B_0 . \tag{9}$$

5.3.2 Solving for Gully Elevation

There are two sets of equations that are fundamental to solving this system. First, it is assumed that if a gully forms, it comes out of the side slope, so that the mouth of the bottom of the gully must intersect the line that forms the top of the side slope. In other words, the equation for the height of the bottom of the gully, evaluated where the gully emerges, must be equal to the elevation of the side slope, evaluated where the mouth of the gully emerges. Written mathematically, this becomes

$$z_{gully}\big|_{L_{mouth}} = z_{SS}\big|_{L_{mouth}} \tag{10}$$

where

> z_{SS} is the elevation of the side slope at any distance L from the break to the ground surface.

The second key equation is that, the volume of cover materials removed by the gully must equal the volume of the material in the fan, following conservation of mass:

$$V_{gully} = V_{fan} . \tag{11}$$

where

> V_{gully} is the volume of the gully in the cover and
> V_{fan} is the volume of the gully in the fan.

In terms of the top slope and side slope, this equation can be written

$$V_{gully}^{TS} + V_{gully}^{SS} = V_{fan} \tag{12}$$

where

> V_{gully}^{TS} is the volume of the gully in the top slope of the cover and
> V_{gully}^{SS} is the volume of the gully in the side slope of the cover.

These equations can be used to express all other unknown variables in terms of the two variables *a* and *h*, which represent the elevation of the mouth of the gully. Using these key equations, the system of equations can be solved for *a* and *h*.

5.3.2.1 Volume of the Gully in the Top Slope of the Cover

As shown in Figure 6 and Figure 7, the cross-sectional area of the gully is assumed to be an isosceles triangle (Willgoose, personal communication, 3 Jan 2011). The height of the triangle is the difference between the height of the top slope and the height of the bottom of the gully. The angle of repose of the gully walls is the angle the gully makes with the horizontal. The base of the triangle is twice the height divided by the tangent of that angle.
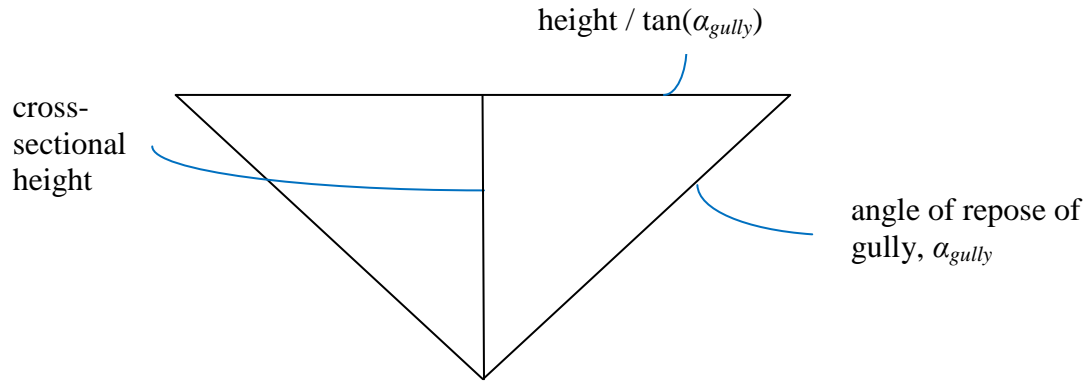
Figure 7. Cross-sectional view of gully

The cross-sectional area of the gully can be represented by

$$A = \frac{1}{2} base \times height \tag{13}$$

$$A = \frac{height \times height}{\tan \alpha_{gully}} \tag{14}$$

and

$$A = \frac{(z_{TS} - z_{gully})^2}{\tan \alpha_{gully}} \tag{15}$$

$$A = \frac{\left[S_{TS}L + z_{ridge} - \left(\frac{a}{b+1} L^{b+1} - B_1 a + S_{TS}L_0 + z_{ridge} \right) \right]^2}{\tan \alpha_{gully}} \tag{16}$$

This equation simplifies to

$$A = \frac{\left(S_{TS}L - \frac{a}{b+1} L^{b+1} + B_1 a - S_{TS}L_0 \right)^2}{\tan \alpha_{gully}} \tag{17}$$

So, the volume of the gully in the top slope is the integral of the cross-sectional area from the initial point of the gully, L_0 to the break between the top slope and the side slope, which corresponds to the length of the top slope, L_{TS}.

$$V_{gully}^{TS} = \int_{L_0}^{L_{TS}} \frac{\left(S_{TS}L - \dfrac{a}{b+1}L^{b+1} + B_1 a - S_{TS}L_0 \right)^2}{\tan\alpha_{gully}} dL \tag{18}$$

Simplifying, the volume becomes

$$V_{gully}^{TS} = \frac{1}{\tan\alpha_{gully}} \int_{L_0}^{L_{TS}} \left[S_{TS}^2 L^2 - \frac{2aS_{TS}}{b+1}L^{b+2} + \frac{a^2}{(b+1)^2}L^{2b+2} + 2(B_1 a - S_{TS}L_0)S_{TS}L - \frac{2a(B_1 a - S_{TS}L_0)}{b+1}L^{b+1} + (B_1 a - S_{TS}L_0)^2 \right] dL \tag{19}$$

$$V_{gully}^{TS} = \frac{1}{\tan\alpha_{gully}} \left[\frac{S_{TS}^2 L^3}{3} - \frac{2aS_{TS}L^{b+3}}{(b+1)(b+3)} + \frac{a^2 L^{2b+3}}{(b+1)^2(2b+3)} + (B_1 a - S_{TS}L_0)S_{TS}L^2 - \frac{2a(B_1 a - S_{TS}L_0)}{(b+1)(b+2)}L^{b+2} + (B_1 a - S_{TS}L_0)^2 L \right]_{L_0}^{L_{TS}} \tag{20}$$

and finally,

$$V_{gully}^{TS} = \frac{1}{\tan\alpha_{gully}} \left[\frac{S_{TS}^2(L_{TS}^3 - L_0^3)}{3} - \frac{2aS_{TS}(L_{TS}^{b+3} - L_0^{b+3})}{(b+1)(b+3)} + \frac{a^2(L_{TS}^{2b+3} - L_0^{2b+3})}{(b+1)^2(2b+3)} \right.$$
$$\left. + (B_1 a - S_{TS}L_0)S_{TS}(L_{TS}^2 - L_0^2) - \frac{2a(B_1 a - S_{TS}L_0)}{(b+1)(b+2)}(L_{TS}^{b+2} - L_0^{b+2}) + (B_1 a - S_{TS}L_0)^2(L_{TS} - L_0) \right] \tag{21}$$

5.3.2.2 Volume of the Gully in the Side Slope of the Cover

The volume of the gully in the side slope is derived in a similar fashion to how the volume was derived for the gully in the top slope. The only differences are that the equation for the line made by the top of the side slope is used instead of the equation of the line made by edge of the top slope, and that the limits of integration are from the edge of the top slope (the break) to the mouth of the gully, at an unknown value, L_{mouth}.

The side slope of the cover can be represented by the line

$$z_{SS} = -\frac{z_{break}}{L_{SS}}L + B_2 \tag{22}$$

where

$$B_2 = \frac{z_{break}}{L_{SS}}(L_{SS} + L_{TS}) \ . \tag{23}$$

The volume of the gully in the side slope is the integral of the cross-sectional area of the gully in the side slope between the break (L_{TS}) and the distance at which the gully mouth comes out the side slope (L_{mouth}).

$$V_{gully}^{SS} = \int_{L_{TS}}^{L_{mouth}} \frac{\left[\left(-\frac{z_{break}}{L_{SS}}L + B_2\right) - \left(\frac{a}{b+1}L^{b+1} + (B_0 - aB_1)\right)\right]^2}{\tan\alpha_{gully}} dL \tag{24}$$

$$V_{gully}^{SS} = \frac{1}{\tan\alpha_{gully}} \int_{L_{TS}}^{L_{mouth}} \left(-\frac{z_{break}}{L_{SS}}L - \frac{a}{b+1}L^{b+1} + (aB_1 - B_0 + B_2)\right)^2 dL \tag{25}$$

Simplifying, the volume becomes

$$V_{gully}^{SS} = \frac{1}{\tan\alpha_{gully}} \int_{L_{TS}}^{L_{gully}} \left(\frac{z_{break}^2}{L_{SS}^2}L^2 + \frac{2az_{break}}{L_{SS}(b+1)}L^{b+2} + \frac{a^2}{(b+1)^2}L^{2b+2} - 2\frac{z_{break}}{L_{SS}}(aB_1 - B_0 + B_2)L \right.$$
$$\left. - \frac{2a(aB_1 - B_0 + B_2)}{b+1}L^{b+1} + (aB_1 - B_0 + B_2)^2 \right) dL \tag{26}$$

$$V_{gully}^{SS} = \frac{1}{\tan\alpha_{gully}} \left[\frac{z_{break}^2}{L_{SS}^2}\frac{L^3}{3} + \frac{2az_{break}L^{b+3}}{L_{SS}(b+1)(b+3)} + \frac{a^2 L^{2b+3}}{(b+1)^2(2b+3)} - \frac{z_{break}}{L_{SS}}(aB_1 - B_0 + B_2)L^2 \right.$$
$$\left. - \frac{2a(aB_1 - B_0 + B_2)}{(b+1)(b+2)}L^{b+2} + (aB_1 - B_0 + B_2)^2 L \right]_{L_{TS}}^{L_{gully}} \tag{27}$$

and finally,

$$V_{gully}^{SS} = \frac{1}{\tan\alpha_{gully}} \left[\frac{z_{break}^2}{L_{SS}^2}\frac{(L_{gully}^3 - L_{TS}^3)}{3} + \frac{2az_{break}(L_{gully}^{b+3} - L_{TS}^{b+3})}{L_{SS}(b+1)(b+3)} + \frac{a^2(L_{gully}^{2b+3} - L_{TS}^{2b+3})}{(b+1)^2(2b+3)} \right.$$
$$\left. - \frac{z_{break}}{L_{SS}}(aB_1 - B_0 + B_2)(L_{gully}^2 - L_{TS}^2) - \frac{2a(aB_1 - B_0 + B_2)}{(b+1)(b+2)}(L_{gully}^{b+2} - L_{TS}^{b+2}) + (aB_1 - B_0 + B_2)^2(L_{gully} - L_{TS}) \right] \tag{28}$$

5.3.2.3   Volume of the Fan

The fan comes from the mouth of the gully, lies along the side slope, and continues to the ground surface (Figure 6). Figure 8 shows a 3-dimensional view of the fan. Figure 9 depicts a birds-eye view of the fan, looking through the fan to the bottom footprint of the fan. The base of the fan is the circular segment. The triangular area is the shadow of the part of the fan that lies on the surface of the side slope. The apex of the fan represents the point of the bottom of the gully mouth.
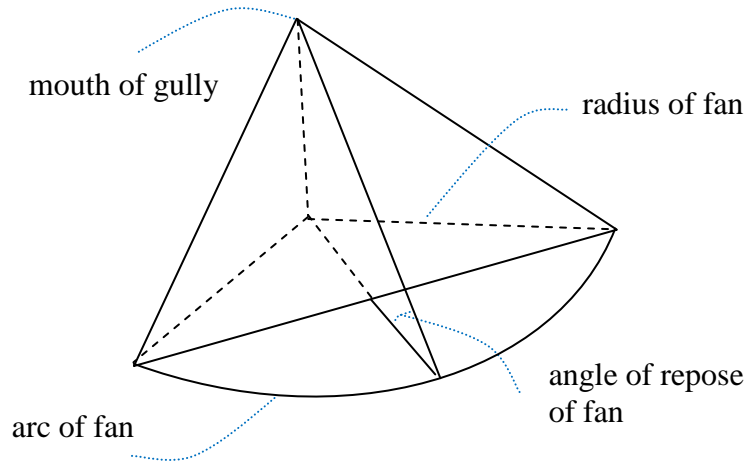
Figure 8. Perspective view of the fan.

Figure 9. Plan view of the fan footprint geometry.
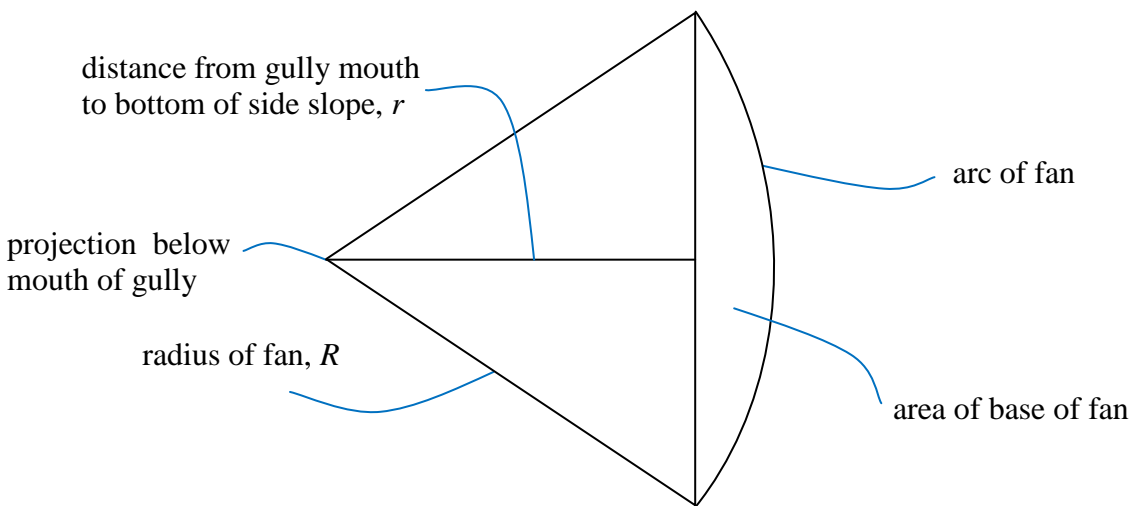
The fan is treated as a pyramidal structure. As such, the volume of the fan corresponds to 1/3 the area of the base multiplied by the height:

$$V_{fan} = \frac{1}{3} Area_{base} \times height \tag{29}$$

For this fan, the area of the base is the area of the circular segment (Figure 9):

$$Area_{base} = R^2 \cos^{-1}\left(\frac{r}{R}\right) - r\sqrt{R^2 - r^2} \tag{30}$$

where

> R is the radius of the fan, and
>
> r is the horizontal distance from the gully mouth to the bottom, or ground surface, of the side slope.

For more information on understanding this area calculation, see Weisstein (2011a) for example.

The radius of the fan can be expressed in terms of the angle of repose of the fan, as shown in Figure 6 and Figure 8.

$$R = \frac{h}{\tan \alpha_{fan}} \tag{31}$$

where

> h is the height of the mouth of the gully, and
>
> α_{fan} is the angle of repose of the fan.

Similarly, the distance r from the gully mouth to the outer edge of the side slope is

$$r = \frac{h}{\tan \alpha_{SS}} \tag{32}$$

where

> α_{SS} is the angle the side slope makes with the ground surface.

The volume of fan can now be expressed in terms of the area in Eq. (30), with new expressions for R and r, and the height to the mouth of the gully, h:

$$V_{fan} = \frac{h}{3} \left[\frac{h^2}{\tan^2 \alpha_{fan}} \cos^{-1}\left(\frac{\frac{h}{\tan \alpha_{SS}}}{\frac{h}{\tan \alpha_{fan}}} \right) - \frac{h}{\tan \alpha_{SS}} \sqrt{ \frac{h^2}{\tan^2 \alpha_{fan}} - \frac{h^2}{\tan^2 \alpha_{SS}} } \right]. \tag{33}$$

Simplifying yields

$$V_{fan} = \frac{h^3}{3} \left[\frac{1}{\tan^2 \alpha_{fan}} \cos^{-1}\left(\frac{\tan \alpha_{fan}}{\tan \alpha_{SS}} \right) - \frac{1}{\tan \alpha_{SS}} \sqrt{ \frac{1}{\tan^2 \alpha_{fan}} - \frac{1}{\tan^2 \alpha_{SS}} } \right]. \tag{34}$$

5.3.2.4   Expressing *a* in terms of *h*

The components for Eq. (11) are now given by the volume of the gully in the top slope (Eq. (21)), the volume of the gully in the side slope (Eq. (28)), and the volume of the fan (Eq. (33)). Next, Eq. (10) can be expanded to express *a* in terms of *h*, the height of the gully:

$$\frac{a}{b+1}L_{mouth}^{b+1} - B_1 a + z_0 = -\frac{z_{break}}{L_{SS}}L_{mouth} + \frac{z_{break}}{L_{SS}}(L_{SS} + L_{TS}) \, . \tag{35}$$

This can be solved for *a* so that

$$a = \frac{\dfrac{z_{break}}{L_{SS}}L_{mouth} - \dfrac{z_{break}}{L_{SS}}(L_{SS} + L_{TS}) + z_0}{B_1 - \dfrac{1}{b+1}L_{mouth}^{b+1}} \, . \tag{36}$$

To express *a* in terms of *h*, an equation for L_{mouth} is used, based on Figure 6, so that

$$L_{mouth} = L_{SS} + L_{cap} - \frac{h}{\tan \alpha_{SS}} \, . \tag{37}$$

Now there are sufficient equations to solve for *h,* and all other variables can be re-written as a function of *h*. The equation for the elevation of the gully bottom can then be computed at any point along the gully.

5.4   Implementation in the Clive DU PA Model

The gully calculations presented above are used in the Clive DU PA Model to allow the formation of a gully that can be different for each realization, based on four stochastic parameters: the gully slope exponent *b*, angles of repose of the gully and fan, and the distance from the ridge of the cover to the initial point of the gully. The model checks to see if the gully is deep enough to get into the waste. If it is, then waste material is assumed to cover the surface area of the fan, and the surface area of the exposed waste is calculated. In order to simplify the calculation, waste concentrations are averaged over the waste layers exposed and then assigned to an exposure area that corresponds to the surface area of the fan plus the area of the waste exposed within the gully.

A random number of gullies sampled from a discrete distribution is chosen to occur, simply to evaluate the effect a variable number of gullies would have on dose. Each of these gullies is identical for a given realization, in order to keep the gully model simple. The fraction of the cover surface area that is consumed by gullies is calculated in order to determine if the quantity of erosion is physically reasonable for an intact embankment.

5.4.1 Performing the Numerical Solution in GoldSim

GoldSim allows the user to iteratively solve a system of equations, such as what is given above, using Newton's method. This numerical solution is implemented in the Clive DU PA Model using a Previous Value element and a looping Container for which the user specifies a maximum number of loop counts and/or a convergence criterion.

Newton's method is a successive approximation method that can be used on differentiable functions. In the Model, it is the height of the gully mouth that is the function of interest. The formula for Newton's method in terms of gully height is

$$h_{n+1} = h_n - \frac{f(h_n)}{f'(h_n)} \, . \tag{38}$$

where

> $f(h)$ is the difference between the volume of the gully and the volume of the fan and
> $f'(h)$ is the derivative of the function $f(h)$.

New values are calculated for h until the difference between h_{n+1} and h_n is sufficiently small. In the Clive DU PA Model, a convergence criterion of 0.01 m^3 is used, such that the difference between the volume of the gully and the volume of the fan is less than 0.01 m^3.

5.4.2 Representation of Gully and Waste

The biggest concern about gullies is whether or not a gully gets deep enough to expose and remove waste and how much waste is exposed and removed. In the current Clive DU PA Model, waste is buried only under the top slope, so the quantity of concern is the distance from the ridge that the gully gets into the waste. In similar terminology to that used above, this variable can be called L_{gully}, where L_{gully} is a vector of distances from the ridge of the cover to where the gully enters the waste layer.

Some assumptions need to be made to allow for a simple calculation of L_{gully}. The column of waste and cover, as modeled in the Clive DU PA Model, is a 1-dimensional representation of the cover, but, the gully model is a 2-dimensional representation, in order to include the slope of the cover surface in the gully calculations. To calculate L_{gully} and the gully outwash of each waste layer, the 2-D representation must be merged with the 1-D representation. Figure 10 illustrates the potential configurations that were considered in the calculation of gully outwash volume and the calculation of where the gully first gets into the waste. The top slope has waste layers (outlined in green) with a cover covering the waste layers. The side slope comes off the top slope, with the break in slope being the vertical dotted black line. The fan leans against the side slope on the right side of the illustrations in Figure 10. The gully (drawn in black) intersects the cover and waste layers.
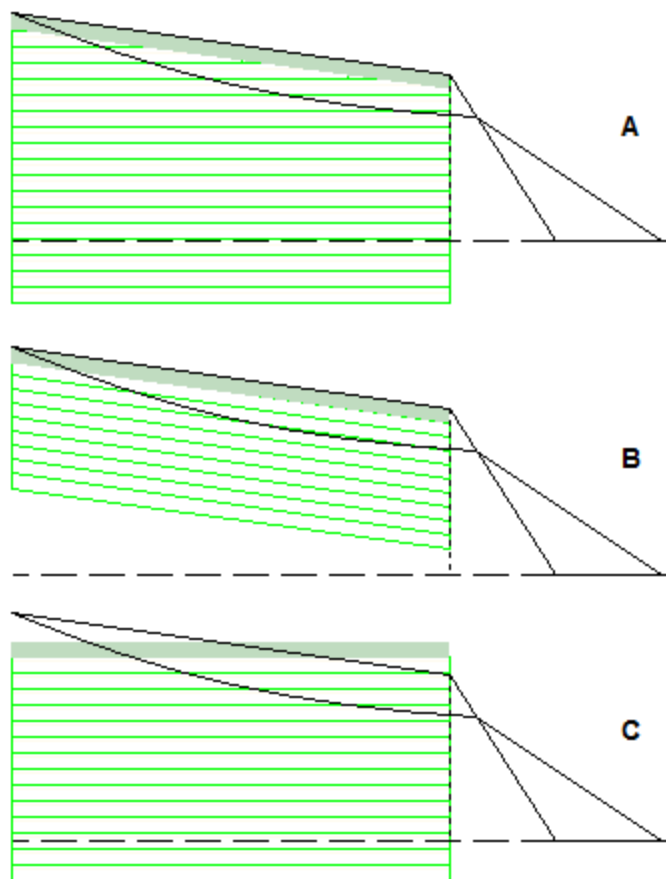
Figure 10. Gully and waste configurations for the gully outwash volume calculation. The cover is represented by the solid green layer and the waste layers outlined in green. A. the embankment as constructed; B. representation of the 1-D column, preserving the slope of the cover throughout the column; C. representation of the 1-D column, preserving the horizontal layering of the waste.

Three different representations were considered in order to model the intersection of waste with the gully and the gully outwash volume of waste. Figure 10A roughly depicts the embankment as it is intended to be constructed, with the cover (solid gray-green) over horizontal waste layers and a sloping top cover. This representation is difficult to implement in the Clive DU PA Model because the waste layers do not continue across the entire top slope of the cover. Figure 10B represents the waste layers continuing for the length of the cover, at the same slope of the top slope of the cover. The problem with this approach is that the gully can dip into and out of a waste layer, meaning that there are two points in each waste layer that the gully could potentially intersect, rather than one intersection point. With this arrangement, there is considerable computational effort required to ensure that the numerical solution for the volume from each layer converges. Figure 10C shows how the implementation of the gully was chosen for the Clive DU PA Model. The top of the cover and top of each waste layer is set as the midpoint of each layer in the top slope of the cover. With the horizontal waste layers, the gully intersects each layer only once.

A problem with implementation of the arrangement in Figure 10C is that the top waste layers at the break in slope in this 1-D representation are higher than the actual cover height at the break in the 2-D representation. So the calculation is an approximation of how many waste layers are cut into by the gully and how much waste is washed out by the gully from each waste layer. This approximation is considered reasonable since the overall gully model is a simplification. Furthermore, if there is sufficient fill material between the top of the DU waste and the bottom of the cover, then the effect is negligible. Some caution should be exercised when interpreting output from the gully model if DU waste is disposed within a few meters of the cover.

5.4.3 Calculation of L_{gully}.

To calculate the volume of each waste layer removed by the gully and the surface area of the waste layers exposed by the gully, the distance from the ridge of the top slope to where the gully first intersects each waste layer, L_{gully}, must be calculated. These values are calculated by finding the intersection of the gully with the horizontal lines at the heights above ground surface for each waste layer. In other words, solve Eq. (9) for L such that z_{gully} equals the height of each waste layer, z_{waste} :

$$L_{gully} = \left(\frac{b+1}{a} (z_{waste} + B_1 a - B_0) \right)^{\frac{1}{b+1}}$$
(39)

where

> z_{waste} is a vector of the waste layer heights above ground surface at the mid-point of the top slope of the cover.

Note that this calculation in the Model requires that $B_1 a - B_0$ be a vector expression of length equal to the number of waste layers.

5.4.4 Calculation of Surface Area

The surface area of the fan and the surface area of the waste exposed by the gully are summed and included in exposure area calculations in the dose assessment.

5.4.4.1   Surface Area of Fan

A simplifying assumption is used to approximate the surface area of the depositional fan: The surface area of the fan is a projection onto a horizontal plane. This assumption is reasonable since the fan has such a low angle of repose (see Section 5.2). Figure 9 shows the shape of this projected area.

The area of a circular sector, $Area_{sector}$, can be found by

$$Area_{sector} = \frac{1}{2} R^2 \theta$$
(40)

where

> R is the radius of the circle and
> θ is the angle cut by the circular segment.

The value of R is the same as that in Eq. (31) above. The value of θ is given by

$$\theta = 2\cos^{-1}\left(\frac{r}{R}\right) = 2\cos^{-1}\left(\frac{\frac{h}{\tan\alpha_{SS}}}{\frac{h}{\tan\alpha_{fan}}}\right) = 2\cos^{-1}\left(\frac{\tan\alpha_{fan}}{\tan\alpha_{SS}}\right) \tag{41}$$

where

    r is the horizontal distance from the gully mouth to the outer edge of the side slope, as given in Eq. (32) above.

Thus, the surface area of the fan SA_{fan} can be expressed as

$$SA_{fan} = \frac{h^2}{\tan^2\alpha_{fan}}\cos^{-1}\left(\frac{\tan\alpha_{fan}}{\tan\alpha_{SS}}\right) \tag{42}$$

For more information on understanding this area calculation, see Weisstein, 2011b, for example.

5.4.4.2 Surface Area of Waste Exposed by Gully

To calculate the surface area of each waste layer exposed, the cross sectional distance of waste exposed by the gully is integrated over the length of the gully in the top slope (see Figure 11).
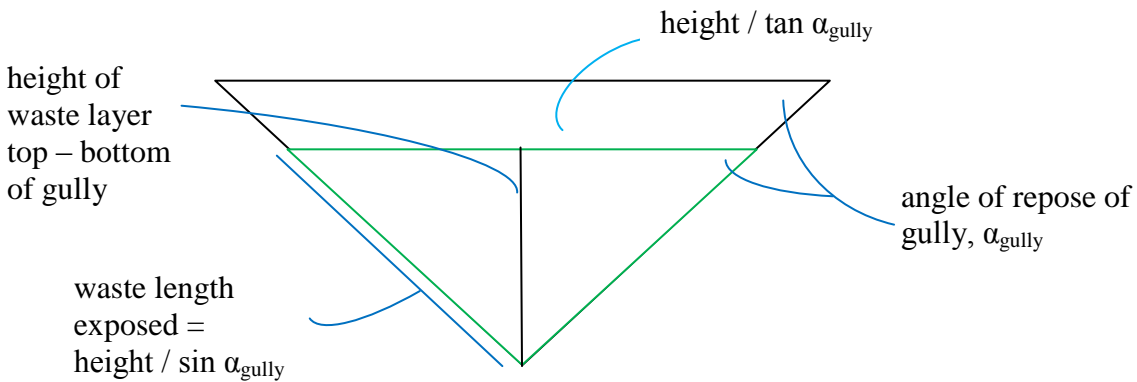

Figure 11. Gully cross section for waste exposure calculations.

The surface area exposed by the gully for each waste layer can be calculated by first calculating the surface area exposed by the gully from the top of each waste layer to the bottom of the gully and then subtracting that calculation from each waste layer. In other words,

$$SA_{WasteLayer1} = SA_{WasteLayer1\_to\_GullyBottom} - SA_{WasteLayer2\_to\_GullyBottom} \tag{43}$$

The surface area exposed from the top of each waste layer to the gully bottom is

$$SA = \frac{2}{\sin \alpha_{gully}} \int_{L_{waste}}^{L_{TS}} (z_{waste} - z_{gully}) dL \tag{44}$$

where the 2 comes from having two sides of the gully exposed.

Substituting in for z_{gully}

$$SA = \frac{2}{\sin \alpha_{gully}} \int_{L_{waste}}^{L_{TS}} \left[z_{waste} - \left(\frac{a}{b+1} L^{b+1} - B_1 a + B_0 \right) \right] dL \tag{45}$$

Simplifying yields

$$SA = \frac{2}{\sin \alpha_{gully}} \left[\left(z_{waste} + B_1 a - B_0 \right)(L_{TS} - L_{waste}) - \frac{a}{(b+1)(b+2)} (L_{TS}^{b+2} - L_{waste}^{b+2}) \right] \tag{46}$$

This value of surface area is then evaluated for each waste layer and used as in Eq. (43) to calculate the surface area exposed for each waste layer. The bottom waste layer surface area is simply the value given in Eq. (46).

5.4.5 Calculation of Volume of Waste Layers Removed

In a similar fashion to the calculation for the surface area of waste exposed by the gully, the volume of each waste layer removed by the gully is calculated by first calculating the volume of waste removed from the top of each waste layer to the bottom of the gully. Then that volume calculation is subtracted from the layer below, similar to Eq. (43):

$$VolWaste_{WasteLayer1} = VolWaste_{WasteLayer1\_to\_GullyBottom} - VolWaste_{WasteLayer2\_to\_GullyBottom} \tag{47}$$

The cross-sectional area of the waste exposed by the gully, similar to Eq. (14), is integrated over the length of the gully that incises the waste.

$$Vol = \frac{1}{\tan \alpha_{gully}} \int_{L_{waste}}^{L_{TS}} (z_{waste} - z_{gully})^2 dL \tag{48}$$

Simplifying,

$$Vol = \frac{1}{\tan \alpha_{gully}} \int_{L_{waste}}^{L_{TS}} (z^2_{waste} - 2z_{waste}z_{gully} + z^2_{gully}) dL \tag{49}$$

$$Vol = \frac{1}{\tan \alpha_{gully}} \int_{L_{waste}}^{L_{TS}} \left[z^2_{waste} - 2z_{waste} \left(\frac{a}{b+1} L^{b+1} - B_1 a + B_0 \right) - \frac{a^2}{(b+1)^2} L^{2b+2} \right.$$
$$\left. + \frac{2aL^{b+1}}{b+1}(B_0 - B_1 a) + (B_0 - B_1 a)^2 \right] dL \tag{50}$$

$$Vol = \frac{1}{\tan \alpha_{gully}} \int_{L_{waste}}^{L_{TS}} \left[z^2_{waste} + 2z_{waste}B_1a - 2z_{waste}B_0 + (B_0 - B_1a)^2 \right.$$

$$\left. - \frac{2z_{waste}a}{b+1}L^{b+1} + \frac{2a(B_0 - B_1a)}{b+1}L^{b+1} + \frac{a^2}{(b+1)^2}L^{2b+2} \right] dL \tag{51}$$

$$Vol = \frac{1}{\tan \alpha_{gully}} \left[\left(z^2_{waste} + 2z_{waste}B_1a - 2z_{waste}B_0 + (B_0 - B_1a)^2 \right)(L_{TS} - L_{waste}) \right.$$

$$- \left(\frac{2z_{waste}a}{(b+1)(b+2)} + \frac{2a(B_0 - B_1a)}{(b+1)(b+2)} \right)(L_{TS}^{b+2} - L_{waste}^{b+2})$$

$$\left. + \frac{a^2}{(b+1)^2(2b+3)}(L_{TS}^{2b+3} - L_{waste}^{2b+3}) \right] \tag{52}$$

This calculation of volume is then evaluated for each waste layer and used as in Eq. (47) to calculate the volume of waste removed by the gully for each waste layer. The bottom waste layer volume is simply that value given in Eq. (52) evaluated for the last waste layer.

5.4.6 Concentration of Waste Removed by Gully

The concentration of waste removed by the gully is averaged and is assumed to be spread out uniformly over the surface area of the fan. This same averaged concentration of waste is assumed to be present in the surface area exposed by the gully.

To obtain the average waste concentration, the concentration of each radionuclide species is computed as a mass-weighted average. The volume of each layer of waste removed by the gully is multiplied by the bulk density of that waste layer to get the mass of waste removed in each layer. Then the mass in each layer is divided by the total mass of waste removed. The mass of each radionuclide in each waste cell is converted to a mass concentration and then multiplied by the mass fraction of each layer removed by the gully. The concentration of waste removed by the gully is then the sum of each radionuclide over every waste layer. It is this total concentration that is used in the dose calculations.

6.0 References

Clover, Thomas J. Pocket Ref. Littleton, Colorado: Sequoia Publishing, Inc., 1998, referenced in Wikipedia definition for Angle of repose, http://en.wikipedia.org/wiki/Angle_of_repose#cite_ref-3

Energy*Solutions*, 2009. *License Amendment Request: Class A South/11E.(2) Embankment.* Revision 1, June 9, 2009.

GTG (GoldSim Technology Group), 2011. *GoldSim: Monte Carlo Simulation Software for Decision and Risk Analysis*, http://www.goldsim.com

NRC, 2010. Workshop on Engineered Barrier Performance Related to Low-Level Radioactive Waste, Decommissioning, and Uranium Mill Tailings Facilities. Nuclear Regulatory Commission. August 3 – 5.

Weisstein, E. 2011a, May 18. Circular Segment. Wolfram Research. Retrieved 23 May 2011 from http://mathworld.wolfram.com/CircularSegment.html.

Weisstein, E. 2011b, May 18. Circular Sector. Wolfram Research. Retrieved 23 May 2011 from http://mathworld.wolfram.com/CircularSector.html.

Willgoose, G. 2005. User Manual for SIBERIA (Version 8.30). Telluric Research. http://www.telluricresearch.com/siberia_8.30_manual.pdf

Willgoose, G. 2010. *Assessment of the Erosional Stability of Covers at Millennial Timescales: Capabilities, Issues and Needs*. Workshop on Engineered Barrier Performance Related to Low-Level Radioactive Waste, Decommissioning, and Uranium Mill Tailings Facilities. Nuclear Regulatory Commission. August 3 – 5.

Willgoose, G. R., and S. Sharmeen, 2006. A one-dimensional model for simulating armouring and erosion on hillslopes. 1. Model development and event-scale dynamics, *Earth Surface Processes and Landforms*, 31: 970-991. http://onlinelibrary.wiley.com/doi/10.1002/esp.1398/abstract